



Swansea University  
Prifysgol Abertawe



## Cronfa - Swansea University Open Access Repository

---

This is an author produced version of a paper published in :  
*Agricultural and Forest Meteorology*

Cronfa URL for this paper:  
<http://cronfa.swan.ac.uk/Record/cronfa23374>

---

### **Paper:**

Sundqvist, E., Persson, A., Kljun, N., Vestin, P., Chasmer, L., Hopkinson, C. & Lindroth, A. (2015). Upscaling of methane exchange in a boreal forest using soil chamber measurements and high-resolution LiDAR elevation data. *Agricultural and Forest Meteorology*, 214-215, 393-401.  
<http://dx.doi.org/10.1016/j.agrformet.2015.09.003>

---

This article is brought to you by Swansea University. Any person downloading material is agreeing to abide by the terms of the repository licence. Authors are personally responsible for adhering to publisher restrictions or conditions. When uploading content they are required to comply with their publisher agreement and the SHERPA RoMEO database to judge whether or not it is copyright safe to add this version of the paper to this repository.

<http://www.swansea.ac.uk/iss/researchsupport/cronfa-support/>

1 **Upscaling of methane exchange in a boreal forest using soil chamber measurements and**  
2 **high-resolution LiDAR elevation data**

3

4 E. Sundqvist<sup>1</sup>, A Persson<sup>1</sup>, N. Kljun<sup>2,3</sup>, P. Vestin<sup>1</sup>, L. Chasmer<sup>4</sup>, C.Hopkinson<sup>4</sup>, A. Lindroth<sup>1</sup>

5

6 <sup>1</sup>Department of Physical Geography and Ecosystem Science, Lund University, Sweden

7 <sup>2</sup>Department of Geography, Swansea University, United Kingdom

8 <sup>3</sup>Centre for Studies of Carbon Cycle and Climate Interactions (LUCCI), Department of Physical  
9 Geography and Ecosystem Science, Lund University, Sweden

10 <sup>4</sup>Department of Geography, University of Lethbridge, Alberta, Canada

11

12 Corresponding author:

13 Elin Sundqvist

14 Department of physical geography and ecosystem science, Lund University

15 Sölvegatan 12

16 223 62 Lund

17 Sweden

18

19 Phone: +46 46 2229759

20 Email: [elin.sundqvist@nateko.lu.se](mailto:elin.sundqvist@nateko.lu.se)

21

22

23

24 **Abstract**

25 Forest soils are generally considered to be net sinks of methane (CH<sub>4</sub>), but CH<sub>4</sub> fluxes vary  
26 spatially depending on soil conditions. Measuring CH<sub>4</sub> exchange with chambers, which are  
27 commonly used for this purpose, might not result in representative fluxes at site scale.  
28 Appropriate methods for upscaling CH<sub>4</sub> fluxes from point measurements to site scale are  
29 therefore needed. At the boreal forest research site, Norunda, chamber measurements of soils and  
30 vegetation indicate that the site is a net sink of CH<sub>4</sub>, while tower gradient measurements indicate  
31 that the site is a net source of CH<sub>4</sub>. We investigated the discrepancy between chamber and tower  
32 gradient measurements by upscaling soil CH<sub>4</sub> exchange to a 100 ha area based on an empirical  
33 model derived from chamber measurements of CH<sub>4</sub> exchange and measurements of soil  
34 moisture, soil temperature and water table depth. A digital elevation model (DEM) derived from  
35 high-resolution airborne Light Detection And Ranging (LiDAR) data was used to generate  
36 gridded water table depth and soil moisture data of the study area as input data for the upscaling.  
37 Despite the simplistic approach, modeled fluxes were significantly correlated to four out of five  
38 chambers with  $R > 0.68$ . The upscaling resulted in a net soil sink of CH<sub>4</sub> of  $-10\mu\text{mol m}^{-2}\text{h}^{-1}$ ,  
39 averaged over the entire study area and time period (June-September, 2010). Our findings  
40 suggests that additional contributions from CH<sub>4</sub> soil sources outside the upscaling study area and  
41 possibly CH<sub>4</sub> emissions from vegetation could explain the net emissions measured by tower  
42 gradient measurements.

43

44 **Keywords:** methane (CH<sub>4</sub>) fluxes, water table depth, topographic wetness index, soil moisture,  
45 soil temperature, methane consumption

## 46 **1. Introduction**

47 The only well characterized biospheric sink for CH<sub>4</sub> is oxidation by methanotrophic bacteria in  
48 soil (Harriss et al., 1982). Globally, this soil CH<sub>4</sub> sink was estimated to range between 28 and 32  
49 Tg CH<sub>4</sub> yr<sup>-1</sup>, which amounts to around 5% of the destruction of CH<sub>4</sub> by OH radicals in the  
50 troposphere (Kirschke, 2013). Forest soils are generally considered to be net sinks of CH<sub>4</sub> with  
51 higher uptake rates than grassland and arable land (Boeckx et al., 1997; Dutaur and Verchot,  
52 2007). However, CH<sub>4</sub> production by archeans usually dominates in anaerobic forest soil  
53 environments such as waterlogged soils (Christiansen et al., 2012; Jungkunst et al., 2008;  
54 McNamara et al., 2006). CH<sub>4</sub> production also takes place in well-aerated soils at anaerobic micro  
55 sites (Fischer and Hedin, 2002; Kammann et al., 2009) and in deeper soil layers where anaerobic  
56 conditions occur (Kammann et al., 2001). Hence consumption and production can occur  
57 simultaneously at one location and soil conditions will determine the direction of the net flux.  
58 Vegetation might also contribute to the CH<sub>4</sub> exchange of a forest. Trees have been found to  
59 transport CH<sub>4</sub> originating from soil water and to release it through the stem or foliage (Terazawa  
60 et al. 2007; Gauci 2010). Aerobic formation of CH<sub>4</sub> in green plants has also been observed  
61 (Keppler et al. 2006; Vigano et al. 2008), although the mechanisms governing plant CH<sub>4</sub> release  
62 are still discussed (Bruhn et al., 2012) and there is little evidence of plant emissions of CH<sub>4</sub> from  
63 in-situ studies (Sundqvist et al., 2012). On the contrary, Sundqvist et al. (2012) found evidence  
64 for plant uptake of atmospheric CH<sub>4</sub> from measurements on spruce, pine, birch and rowan in a  
65 boreal forest.

66 Soil CH<sub>4</sub> flux rates also vary considerably both spatially and temporally (Christiansen et  
67 al., 2012; Ishizuka et al., 2009; Konda et al., 2008; Lessard et al., 1994; Reay et al., 2005; Yu et  
68 al., 2008). Spatial variability in soil CH<sub>4</sub> fluxes can be due to variability in soil moisture, soil

69 texture, and water table depths, factors that are dependent on topography, vegetation, and soil  
70 type, for example. Soil moisture (Castro et al., 1994; Guckland et al., 2009; Lessard et al., 1994)  
71 and soil texture (Dorr et al., 1993; Dutaur and Verchot, 2007; Ishizuka et al., 2009) alters soil  
72 diffusivity, which controls the rate at which atmospheric CH<sub>4</sub>, and oxygen are supplied to the  
73 bacteria. Water table depth alters the relative extent of aerobic and anaerobic zones in soils. A  
74 rise of the water table leads to a decreased oxic soil zone and thus reduced CH<sub>4</sub> uptake  
75 (Kammann et al., 2001; Roulet et al., 1992). Changes in soil temperature and precipitation are  
76 also responsible for temporal variability in CH<sub>4</sub> exchange. Increases in temperature stimulate the  
77 activity of both methanogens (Yvon-Durocher et al., 2014) and methanotrophs (Crill et al., 1994;  
78 King and Adamsen, 1992), although methanogens benefit more (Dunfield et al., 1993). Other  
79 factors that have been found to influence soil CH<sub>4</sub> exchange in forests are soil pH (Weslien et al.,  
80 2009) and nitrogen availability (Stuedler et al., 1989).

81         In situ chamber measurements and soil incubations in laboratories have long been the  
82 dominant methods for studying CH<sub>4</sub> exchange in forests, although larger scale  
83 micrometeorological methods are gaining in popularity (Nicoloni et al., 2013). While CH<sub>4</sub>  
84 exchange occurs and is often measured at the centimeter scale, it varies globally, and has a  
85 significant influence on biospheric-atmospheric interactions and feedbacks associated with  
86 climatic change (Schimel and Potter, 1995). Appropriate upscaling of CH<sub>4</sub> exchange from  
87 chamber-based point measurements will allow scientists to better understand the contribution of  
88 methane from soil and plant environments measured using eddy covariance/micrometeorological  
89 methods with extension to model estimates of regional to global CH<sub>4</sub> budgets (Hashimoto et al.,  
90 2011; Marushchak et al., 2013; Schimel and Potter, 1995). A few studies have upscaled CH<sub>4</sub>  
91 fluxes using simple extrapolations of chamber measurements or soil incubations from a few

92 locations multiplied by site area. However these methods do not consider the spatial  
93 heterogeneity of forest soil texture or type, or topographical variability, which may greatly  
94 influence wetting and drying regimes, and therefore CH<sub>4</sub> fluxes.

95 Global and regional estimates of soil CH<sub>4</sub> sink strength use soil texture classes (Dorr et al., 1993;  
96 Dutaur and Verchot, 2007), land use type (Grunwald et al., 2012), ecosystem class and/or  
97 climatic zones (Dutaur and Verchot, 2007) to spatially parameterize CH<sub>4</sub> exchanges. However,  
98 regional models often fail to incorporate the spatial heterogeneity within each class, including  
99 fuzzy boundaries between classes. This results in inaccurate characterization of classes, and  
100 especially within the sometimes broad transition zones between classes (Matson et al., 1989).

101 These issues may be overcome by incorporating process-based models of CH<sub>4</sub> consumption  
102 driven by gaseous diffusion or diffusion in combination with microbial activity (Curry, 2007;  
103 Del Grosso et al., 2000; Ridgwell et al., 1999). Some process-based models do not account for  
104 production of CH<sub>4</sub> and are not applicable to soils that seasonally shift from net sinks to net  
105 sources (Del Grosso et al., 2000). Process-based models can become exceedingly complex,  
106 requiring detailed inputs of spatio-temporally varying climate, vegetation and soil  
107 physiochemical properties (Hashimoto et al., 2011). More simple, empirical models have been  
108 developed for site-specific applications. Castro et al (1994) found that soil moisture, as the only  
109 explanatory variable, could satisfactorily predict CH<sub>4</sub> fluxes at locations within a temperate  
110 forest. Christiansen et al. (2012) used spatial variability in soil moisture and water table depths  
111 derived from elevation data to upscale CH<sub>4</sub> fluxes from manual chamber measurements to site  
112 scale at two temperate deciduous forests.

113           At the Norunda boreal forest site in central Sweden, chamber measurements of soils and  
114 vegetation indicate that the site is a net sink of CH<sub>4</sub> (Sundqvist et al., 2012, 2014b), while

115 gradient measurements above the forest canopy indicate that the site is a net source of CH<sub>4</sub>  
116 (Sundqvist et al., 2015). The aim of this study was to quantify soil CH<sub>4</sub> exchange for the entire  
117 site (100 ha) by upscaling soil CH<sub>4</sub> exchange through developing an empirical model for a  
118 mature coniferous forest based on automated chamber observations with a high temporal  
119 resolution, in combination with high-resolution LiDAR elevation data. The model will also serve  
120 as a mean to further examine the discrepancy between results obtained from chamber  
121 measurements and tower gradient measurements. In correspondence to findings of Christiansen  
122 et al. (2012), Fiedler et al. (2005) and Grunwald et al. (2012), we hypothesize that emissions  
123 from wet patches scattered at the site may exceed the uptake in well-aerated parts of the soil and  
124 hence even relatively small source areas may shift a larger area from a sink to a source (Fiedler  
125 et al., 2005).

126

127

## 128 **2. Method**

129

### 130 *2.1 Site description*

131 Upscaling of soil CH<sub>4</sub> exchange was completed for a 100 ha area at the Norunda site, 60°5'N,  
132 17°29'E, in central Sweden from July through September 2010 during coincident chamber and  
133 tower gradient measurements. The Norunda site is situated at the southern edge of the boreal  
134 forest zone and is comprised of 120 years old mixed pine (*Pinus sylvestris*) and spruce (*Picea*  
135 *abies*) trees. The forest was thinned in 2008 within the NE to SW sectors surrounding the  
136 measurement tower to a radius of 200 m, which decreased the leaf area index within this area  
137 from 4.8 to 2.8 m<sup>2</sup>m<sup>-2</sup>. Trees within the SW to NE sectors have not been thinned nor fertilized in  
138 the last few decades. Soil are comprised of glacial till, classified as dystric regosol (Lundin et al.,  
139 1999) and include an organic layer of about 3-10 cm. The area within 500 m radius of the  
140 measurement tower is relatively flat, with elevation ranges from 40-52 m above sea level (Figure  
141 1). Since 1843, the water table in the area has been artificially lowered as a result of several  
142 ditches surrounding the forest. The last known ditch installation was in 1980. Mean air  
143 temperature measured at Uppsala climate station, 30 km south of Norunda, was 6.5° C and mean  
144 precipitation was 576 mm (1980-2010).

145

### 146 *2.2 Instrumentation*

147 In this study, eight CH<sub>4</sub> chambers are used: three chambers (T1-T3) were located in the thinned  
148 section, and five (U1-U5) were located in the undisturbed section of the forest. In areas of  
149 higher water table, CH<sub>4</sub> exchanges were measured, using a single 'floating' chamber positioned  
150 on standing shallow water in the thinned section of the forest.



151 Due to equipment limitations, measurements were conducted at one section at a time and were  
152 averaged from hourly chamber measurements to daily periods from 1 August to 30 September  
153 2009 at the thinned plot, and 7 July to 30 September 2010 at the undisturbed plot. The soil  
154 chambers each had a volume of 110 l and covered a surface-area of 0.2 m<sup>2</sup>. Concentrations in the  
155 chambers were measured for 6 minutes after chamber closure with a high precision off-axis  
156 integrated cavity output spectroscopy laser gas-analyser (DLT-100, Los Gatos Research). A  
157 small fan was installed in each chamber to ensure proper headspace mixing during closure. Air  
158 was circulated between the chamber and a manifold at a flow rate of 8-10 l min<sup>-1</sup>. A sub-sample  
159 of the air stream was passed through the gas analyzer at a flow rate of 1.2 l min<sup>-1</sup>. The rate of  
160 change in CH<sub>4</sub> concentration was determined through a linear fit to the first 2 minutes of  
161 concentration data and averaged over hourly periods. CH<sub>4</sub> fluxes were calculated as

162  $F_{CH_4} = \frac{dC}{dt} \frac{V}{A}$ , where  $C$  (μmol m<sup>-3</sup>), is molar density,  $V$  (m<sup>3</sup>) is chamber volume and  $A$  (m<sup>2</sup>) is

163 the ground surface area covered by the chamber. Only measured fluxes were used for upscaling,  
164 i.e. CH<sub>4</sub> flux data was not gap-filled. For further details on the chamber measurements, see  
165 Sundqvist et al. (2014b). Soil temperature was measured continuously at a depth of 5 cm below  
166 the soil surface within the chambers using type-T thermocouples. Soil moisture was also  
167 measured continuously and averaged within the top 5 cm of the soil within chambers using MI-  
168 2x ThetaProbe from DeltaT Devices and at additional positions throughout the study area.

169

### 170 *2.3 Empirical model for upscaling of CH<sub>4</sub> exchange*

171 Upscaling of soil CH<sub>4</sub> exchanges was derived using a multiple linear regression analyses (Draper  
172 and Smith, 1998) based on typical control variables: soil temperature, soil moisture and water  
173 table depth as they compare with hourly average chamber measurements. The resulting

174 regression model was assumed to be valid as long as the water table was greater than 5 cm below  
175 the soil surface such that an oxic soil zone could enable CH<sub>4</sub> consumption by methanotrophs. For  
176 higher water tables a median value of 40 μmol m<sup>-2</sup>h<sup>-1</sup> obtained from the floating chamber  
177 measurements was used. The mean value of the floating chamber was as large as 120 μmol m<sup>-2</sup>h<sup>-1</sup>  
178 due to several (>1000 μmol m<sup>-2</sup>h<sup>-1</sup>) flux values, possibly related to ebullition. Different  
179 combinations of chamber measurement were tested when the empirical model was derived  
180 through regression analyses. Three chambers were always used for model development while the  
181 other five were used for model evaluation. The model that showed the best fit between input data  
182 and regression curve and best predicted fluxes was selected for upscaling. Sensitivity analyses of  
183 model parameters were made by local sensitivity analyses by varying one variable at the time  
184 and keeping the other fixed (Hamby, 1994). Each parameter was changed by 20% at the time and  
185 the change in the model output was quantified.

186

#### 187 *2.4 Model input*

188 For upscaling of soil CH<sub>4</sub> exchange to site level, spatial information on soil moisture, water table  
189 depth and soil temperature were needed as input. Daily average soil temperatures at the site were  
190 relatively constant in space, hence only temporal variations in temperature were accounted (Table  
191 1). Spatial information of soil moisture and water table depth were estimated using airborne-  
192 LiDAR data collected in June 2011.

193 LiDAR point cloud data were first classified to ground and non-ground returns using  
194 TerraScan (TerraSolid, Inc.). Ground-classified returns were rasterized using an inverse  
195 distance weighted algorithm (Hopkinson et al., 2005) to generate a digital elevation model  
196 (DEM) with a cell resolution of 1 m (Figure 1). A topographic wetness index (TWI) was derived

197 from the DEM (Beven and Kirkby, 1979), and used to estimate unsaturated zone soil moisture  
198 according to Lin et al., (2006), Schmidt and Persson, (2003), and Western et al., (1999). Further,  
199 Beldring et al., (1999) demonstrated that within some forested areas, the spatial patterns of soil  
200 moisture can be estimated more accurately using topography than with other hydrological state  
201 measurements, as the latter are often too variable when used with sparsely distributed  
202 measurements. TWI is calculated as  $TWI = \ln(A / \tan \beta)$ , where A is the upslope area ( $m^2$ ) being  
203 drained through the position of interest, and  $\beta$  is the slope angle (degrees) of that position  
204 (Beven and Kirkby, 1979). In the present study, the flow routing and the drainage area (A) have  
205 been calculated in a multiple flow direction algorithm that takes the shape of the slope into  
206 account (Pilesjö et al., 1998; 2006). TWI was converted to soil moisture based on the linear  
207 regression between TWI and soil moisture measured at 12 site locations in 2010 (Figure 2). TWI  
208 was also compared with soil moisture measured in 2013 as a separate evaluation of TWI as a  
209 proxy for soil moisture at the site. Soil moisture data in 2013 were sampled at several positions  
210 as oppose to other years (Figure 2).

211 The DEM was also used to estimate the spatial variability of water table depths based on  
212 the assumption that topographically low areas are likely to have water table depths nearer to the  
213 surface than topographically higher positions (e.g. Lamb et al., 2001, Molénat et al., 2005,  
214 Seibert et al., 1997).

215 Since continuous measurements of water table depth were available only at a single location in  
216 the study area a smoothed ground surface was used to represent the water table. The smoothed  
217 ground surface area was lowered in each cell with the water table depth obtained from the one  
218 measurement location. The elevation values' spatial autocorrelation were plotted in semi-  
219 variograms in which the spatial dependency of elevation was estimated. The geomorphology of

220 the area was studied in aerial imagery and within the DEM. The average measure from valley  
221 bottom to hilltop to valley bottom of the ground surface and the results of the spatial auto-  
222 correlation formed the base of the smoothing process. The smoothed ground surface was  
223 obtained by applying a low-pass filter that averaged the elevation values up to a distance where  
224 the spatial auto-correlation of elevation declined.

225 Validation of the spatial distribution of the depth to water table and soil moisture was  
226 determined using LiDAR-derived vegetation heights as a proxy indicator, assuming that trees are  
227 often not as tall in wet soils compared to drier soils (Heiskanen and Makitalo, 2002; Koslowski,  
228 1997; Polacek et al., 2006). Spatial variations in tree heights were determined using a digital  
229 surface model (DSM) derived from LiDAR data. The DSM was determined by gridding the  
230 maximum height of classified non-ground laser pulse returns within a 3 meter search radius and  
231 subtracted from the DEM to determine vegetation height relative to ground surface. The  
232 comparison between tree height and depth to water table and soil moisture could be made for an  
233 area within 250 m radius from the tower where the trees are the same age.

234

### 235 *2.5 Gradient measurements*

236

237 Gradients were measured between 31.7m and 58.5 m, and between 31.7 m and 101.6 m at the main tower  
238 at Norunda with a laser gas analyser (DLT-100, Los Gatos Research). Here we used the gradient  
239 measured between 31.7 m and 58.5 m since footprint analyses using the model by Kljun et al (2004)  
240 showed that these levels were more representative for the upscaled area than the gradient including the  
241 highest level (Sundqvist et al., 2015). Tower CH<sub>4</sub> fluxes were calculated in two different ways; the  
242 combined eddy covariance and gradient method (ECG) and the modified Bowen-ratio method (BR)

243 (Sundqvist et al., 2015). In the ECG method the CH<sub>4</sub> flux is calculated according to Ficks law of  
 244 diffusion:

$$245 \quad F_{CH_4}(ECG) = -\frac{1}{V} K_c \frac{\Delta C}{\Delta z} \quad (1)$$

246

247 where  $V$  ( $m^3 mol^{-1}$ ) is the volume of one mole of air and  $C$  is CH<sub>4</sub> concentration ( $\mu mol mol^{-1}$ ).

248 The turbulent diffusivity  $K_c$  is derived from the Monin Obukhov similarity theory,

$$249 \quad K_c = \frac{ku_*\Delta z}{\ln \frac{z_2}{z_1} - \psi_t \left( \frac{z_2}{L} \right) + \psi_t \left( \frac{z_1}{L} \right) - \int_z^{z_*} \Phi_t (1 - \phi_t) \frac{dz}{z}} \quad (2)$$

250 where  $k = 0.4$  is von Karman's constant,  $u_*$  ( $m s^{-1}$ ) is friction velocity,  $z_2$  (m) is upper air intake

251 height,  $z_1$  (m) is lower air intake height,  $\Delta z$  is the difference between the intake heights,  $L$  is the

252 Obukhov length and  $\psi_t$  is the diabatic correction function for heat profiles according to

253 Högström (1988).  $u_*$  and  $L$  were obtained from the eddy covariance measurements. The function

254  $\Phi_t$  denotes the diabatic correction function for gradients.  $\Phi_t$  is integrated from the height  $z$

255 inside the roughness sublayer to the top of the roughness sublayer ( $z_* = 35.9$  m). The roughness

256 sublayer effects are expressed through  $\phi_t$  (Mölder et al., 1999; Physick and Garratt, 1995). All

257 heights take the displacement height into account.

258 The modified Bowen ratio method is based on the assumption of identical diffusivities for CO<sub>2</sub>

259 and CH<sub>4</sub> fluxes. If the CO<sub>2</sub> flux ( $F_{CO_2}$ ) is known, e.g., the CH<sub>4</sub> exchange  $F_{CH_4}$  can be derived

260 (Moncrieff et al., 1997) as

$$261 \quad F_{CH_4}(BR) = F_{CO_2} \frac{\Delta C_{CH_4}}{\Delta C_{CO_2}} \quad (3)$$

262 A measurement uncertainty was calculated for each half hourly value based on estimated  
263 uncertainty in the ingoing variables. Assuming independence between the errors, the error in the  
264 mean value for the investigated period was propagated according to the simplified method (Hu,  
265 1966) for both the ECG and BR methods. The statistical uncertainty was calculated as the  
266 standard error of the mean. The total error in the mean was estimated as the sum of these  
267 uncertainties.

## 268 **3. Results**

269

### 270 *3.1 Empirical model*

271 The combination of chamber data used for developing the model had a clear impact on the  
272 goodness of fit of the empirical model (Table 2). This was also the case for the correlation  
273 between modelled fluxes and fluxes from chambers used for evaluation of the model. The model  
274 with best fit ( $R^2$ ) to input data and highest correlation with evaluation data ( $R$ ) was chosen for  
275 upscaling of the  $CH_4$  exchange. The model with the overall best performance had an  $R^2$  of 0.8  
276 and  $R$  values of 0.85, 0.72, 0.94, 0.68 and 0.15 (Table 2) for U1, U2, U5, T1 and T3,  
277 respectively. All  $R$  values except the one for T3 were significant. The model equation for  
278 estimating the net  $CH_4$  exchange ( $CH_{4exchange}$ ) was  $CH_{4exchange} = -0.32T + 3.5W + 0.08SM - I$ ,  
279 where  $T$  is soil temperature,  $W$  is water table depth,  $SM$  is soil moisture and  $I$  is the regression  
280 intercept which equaled  $2.8 \mu\text{mol m}^{-2} \text{h}^{-1}$ .

281 Uptake values ( $\mu\text{mol m}^{-2} \text{h}^{-1}$ ) were overestimated for U1, U5 and T3 and underestimated for U2  
282 (Figure 3). Sensitivity analyses showed that the model was equally sensitive for changes in water  
283 table depth and soil temperature and less sensitive to changes in soil moisture. A 20 % change in  
284 parameter values resulted in 9.1%, 9.2% and 2.7 % change in net  $CH_4$  exchange for water table  
285 depth, soil temperature and soil moisture, respectively.

286

### 287 *3.2 TWI and soil moisture*

288 TWI and soil moisture were positively correlated with  $R$  values ranging from 0.1-0.7 in 2013 and  
289 0.2-0.7 in 2010 (Figures 4a-b). The correlation coefficients were higher on average in 2013  
290 (Figure 4a). Correlations were not significant due to the limited number of soil moisture

291 measurements. P-values for 2010 were generally  $< 0.2$  (Figure 4c). When soil moisture  
292 decreased after precipitation, the correlation between TWI and soil moisture increased slightly  
293 (Figure 4d). Spatio-temporal variability in soil moisture generated from the relationship between  
294 TWI and soil moisture measurements was on average between 14.7- 22.3 % for 96 % of the data  
295 (Figure 5a). Daily input data from soil moisture measurements varied between 5-35 %. A map of  
296 tree heights in the study area is shown in Figure 5b. It can be seen that areas with lower than  
297 average tree heights coincide with areas with higher than average soil moisture in the area within  
298 250 m radius from the tower where trees are the same age. There was a significant correlation  
299 between soil moisture and tree height with a correlation coefficient of  $-0.16$ .

300

### 301 *3.3 Water table depth*

302 For each 1 m by 1 m cell, the spatial dependency of elevation on the water table was estimated to  
303 be 80 m. A water table surface was generated applying a low-pass filter on the DEM that  
304 averaged the elevation values taking 80 m surroundings into account. The ground water  
305 measurements were used to let this filtered water table fluctuate temporarily. Spatio-temporal  
306 variability in water table ranged on average from -5 m below ground to 0.7 m above ground if  
307 excluding outliers, with 2 and 98 percentiles of  $-2.9$  m and  $-0.27$  m. A few wet patches with  
308 standing water are shown in the map of modelled water table depth averaged over the study time  
309 period (Figure 5c). In figure 5b it can be seen that in areas within 250 m from the tower, lower  
310 than average tree heights coincide with areas with higher than average water tables. There was a  
311 significant correlation between depth to water table and tree height with a correlation coefficient  
312 of  $-0.29$ .

313



314

315 *3.4 Upscaled CH<sub>4</sub> exchange*

316 Averaged modelled net CH<sub>4</sub> exchange (derived as described in Section 2.2) of the entire study  
317 area and time period is -10.0 μmol m<sup>-2</sup> h<sup>-1</sup> with a standard deviation of 0.8 μmol m<sup>-2</sup> h<sup>-1</sup>.

318 However, the average CH<sub>4</sub> exchange for the entire measurement period varies spatially between  
319 uptake values of -21 μmol m<sup>-2</sup> h<sup>-1</sup> and the assigned production value of 40 μmol m<sup>-2</sup> h<sup>-1</sup> for areas  
320 with standing water (Figure 5d). Net average emissions are found for 1.75% of the study area.

321 Time series of daily averaged modelled CH<sub>4</sub> exchange, soil moisture, soil temperature and water  
322 table depth are shown in Figure 6. Over the course of the measurement period, net CH<sub>4</sub> uptake  
323 decreased along with decreased soil temperatures.

324

325

326

327

328

329

330

331

## 332 **4. Discussion**

333

### 334 *4.1 Evaluation of model and upscaling*

335 Although the empirical model for upscaling of CH<sub>4</sub> exchange only includes data from three  
336 chamber locations and is driven by the three variables, soil temperature, depth to water table and  
337 soil moisture, this method shows good agreement between modelled and measured fluxes, in  
338 general. However the model is unsuccessful in capturing local deviations in CH<sub>4</sub> flux behavior such as  
339 the peak emission followed by a shift from source to sink of chamber T3 (Figure 3). The peak in CH<sub>4</sub>  
340 emissions may be due to high soil moisture level following precipitation (Sundqvist et al., 2014b), with  
341 the shift to a sink when the soil dries up.

342 Since the model is less sensitive to changes in soil moisture than to changes in water table depth  
343 and soil temperature (cf.Eq.1), soil moisture driven events might not be fully captured.

344 Modelled estimates of soil moisture and water table depths derived from LiDAR data  
345 agrees well with the qualitative picture we have of the study area. Moreover, the shorter trees are  
346 found in areas with higher soil moisture and near surface water table, which support the  
347 hydrological patterns generated from the DEM (Heiskanen and Makitalo, 2002; Koslowski,  
348 1997; Polacek et al., 2006). Future studies should include more measurements of soil moisture  
349 and water table depths covering a larger area for a more quantitative evaluation. It would also be  
350 desirable to evaluate the upscaling by measuring CH<sub>4</sub> fluxes with soil chambers at several  
351 locations in the area.

352

### 353 *4.2 Upscaled CH<sub>4</sub> exchange*

354 The results of the modelled/upscaled soil CH<sub>4</sub> exchange indicates that this forest is an overall  
355 sink of -10.0 μmol m<sup>-2</sup>h<sup>-1</sup>. Even if the assigned production areas of 40 μmol m<sup>-2</sup>h<sup>-1</sup> (for water

356 table depths higher than 5 cm below the soil surface) were extended to all water table depths  
357 higher than 30 cm below the soil surface, the area remained a net sink of  $-9.1 \mu\text{mol m}^{-2}\text{h}^{-1}$ .  
358 According to the chamber measurements, the average  $\text{CH}_4$  exchange for the undisturbed forest  
359 and the thinned forest were  $-10 \mu\text{mol m}^{-2} \text{h}^{-1}$  and  $-5 \mu\text{mol m}^{-2} \text{h}^{-1}$ , respectively (Sundqvist et al.,  
360 2014b), and hence agreed well with the modelled values. Results from the modelled site-wide  
361 water table depth show that 90 % of the area had a water table lower than  $-0.7 \text{ m}$ , which should  
362 be well below the critical levels for net  $\text{CH}_4$  emissions. Christiansen et al. (2012) found that  
363 maintaining a ground water table depth below  $0.5 \text{ m}$  throughout their study area would shift their  
364 site from a source of  $\text{CH}_4$  to a sink of  $\text{CH}_4$ . Assuming that an uptake of  $-10 \mu\text{mol m}^{-2}\text{h}^{-1}$  is  
365 reasonable in well aerated soils, a net production area of more than 20 % of the total area, with  
366 average fluxes of  $40 \mu\text{mol m}^{-2}\text{h}^{-1}$ , would be necessary to shift the site from a sink to a source.  
367 The size of this area would of course decrease if the  $\text{CH}_4$  production rates approached levels of  
368 wetland fluxes. In general, uptake rates decreased from July to September (Figure 6) and it is  
369 possible that additional data from wetter and colder seasons would alter the findings.

370

#### 371 *4.3 Water table depth*

372 We used filtered elevation data derived from LiDAR measurements to derive the general pattern  
373 of the water table in the study area and regulated the absolute depths of the modelled water table  
374 with measurements from one single location. Other studies have modelled water tables from  
375 TWI, which may be related to topography, depending on soil type (Buttle et al. 2004). Siebert et  
376 al. (1997) concluded that one single location of observation of water table depth was sufficient  
377 for the calibration of an index to predict groundwater spatially distributed in a spruce forested  
378 catchment in the West of Sweden. However, we are aware of an area with standing water in

379 summer 2010, which was not accurately captured by the model, although the generated water  
380 table map and soil moisture map show higher than average values for this area. The generation of  
381 the water table depth is based solely on the DEM. In nature, water table depth is also dependent  
382 on soil properties such as large pore structure, impermeable clay layers and sub-surface lateral  
383 flow in hillslopes (Grip and Rodhe, 1994; Ward and Trimble, 2004). Clay layers in Norunda  
384 soils have been observed at a few locations, but their spatial extent and general depth are  
385 unknown.

386 Moreover, the water table map was developed under conditions where the observed water  
387 table depth ranged from 0.9 m-1.7m below soil surface. Jungkunst et al. (2008) found that CH<sub>4</sub>  
388 emissions of a hydromorphic forest soil increased drastically when the water table was 10-20 cm  
389 from the soil surface. Fiedler and Sommer (2000) determined a threshold depth of 15 cm of the  
390 water table for wetland soils; above this threshold, production dominated the CH<sub>4</sub> exchange.  
391 Since the control of CH<sub>4</sub> production at high water tables differs from drivers of CH<sub>4</sub> consumption  
392 and mainly depends on substrate availability and soil temperature (Christensen et al., 2003), an  
393 additional model developed for high water tables might improve the upscaling.

394

#### 395 *4.4 Soil moisture*

396 Observed soil moisture was well represented by the model with variations between 5% and 35%.  
397 However, the average spatial variation of soil moisture generated from TWI was lower. The  
398 porosity of the soil in Norunda is around 40% and in areas with standing water, soil moisture  
399 should reach the value of the porosity. Only 0.5 % of the cells had average soil moisture above  
400 24% and no cells had average values above 31%. These low values may point to the fact that wet  
401 areas with observed standing water were situated in parts of the landscape which are represented

402 as flat or convex in the DEM. The water routing algorithm creates a pattern, which is based only  
403 on the topography. The model might then disperse water over larger areas rather than  
404 concentrating it due to low differences in elevation values. In reality, however, micro-topography  
405 and soil properties may drive the water distribution.

406

#### 407 *4.5 Upscaling soil CH<sub>4</sub> exchange versus gradient measurements*

408 The results from upscaling of soil CH<sub>4</sub> exchange show a net consumption of about -10 μmol m<sup>-2</sup>  
409 h<sup>-1</sup> while the tower gradient measurement indicates the site is a net CH<sub>4</sub> source of about 3.4 μmol  
410 m<sup>-2</sup>h<sup>-1</sup> for the same time period (Sundqvist et al., 2015). The ECG method resulted in a mean  
411 emission of 5.2 ± 0.64 μmol m<sup>-2</sup>h<sup>-1</sup> while the BR method gave 1.6 ± 0.73 μmol m<sup>-2</sup>h<sup>-1</sup>. The errors  
412 of these two methods does not overlap but both indicate that the forest is a source of methane.  
413 The difference between the methods is most likely caused by uncertainty in the methods itself.  
414 Here are many empirical corrections involved especially in the ECG method that might be the  
415 cause of this discrepancy.

416 Unfortunately the uncertainty in the upscaled soil emissions cannot be easily done since we do  
417 not have enough spatial data on e.g. soil properties available. The rough sensitivity analyses  
418 made in section 4.2 is however a strong indication that the soil is a sink of methane and not a  
419 source.

420 The study area included the outskirts of a clear-cut (Figure 2). The water table in this part  
421 of the study area was increased due to decreased evapotranspiration following clear-cutting. The  
422 model did not capture this local effect since water table depth was calculated from elevation data  
423 and a single measurement location within the forest. Chamber measurements on the clear-cut  
424 from October -November 2010 showed average emissions of 15 μmol m<sup>-2</sup>h<sup>-1</sup> (Sundqvist et al.,

425 2015). Emissions from the clear-cut may be part of the reason for the discrepancy between the  
426 upscaled soil chamber data and the gradient measurements. It is also possible that emissions  
427 from the part of the clear-cut located outside of the upscaled boundary and other sources outside  
428 the study area contribute to the tower gradient measurements.

429         The gradient measurements represent the net exchange of CH<sub>4</sub> above the canopy and  
430 hence it is not possible to distinguish fluxes at soil level from an exchange of CH<sub>4</sub> coupled to  
431 vegetation. CH<sub>4</sub> emissions by vegetation (Terazawa et al. 2007; Gauci 2010; Keppler et al. 2006;  
432 Vigano et al. 2008) could partly explain the discrepancy between upscaled chamber data and  
433 gradient measurements, if these contribute significantly to the net CH<sub>4</sub> exchange at Norunda.  
434 However, so far only a net uptake of CH<sub>4</sub> by vegetation has been measured at a few locations at  
435 Norunda (Sundqvist et al. 2012).

436

### 437 *5 Conclusions*

438 A simple empirical model for upscaling of soil CH<sub>4</sub> exchange at a boreal forest site was  
439 developed from chamber measurements, driven by soil temperature, water table depth and soil  
440 moisture. High resolution LiDAR elevation data formed the basis for the mapping of water table  
441 depth and soil moisture of the study area, while vegetation heights were used as a proxy indicator  
442 for spatial variations of average soil moisture regime. A significant correlation was found  
443 between the topographical wetness index (TWI) derived from the LiDAR data and soil moisture  
444 measured at the study area, which enabled a conversion of TWI to soil moisture. Modelled CH<sub>4</sub>  
445 fluxes were in good agreement with measured fluxes at four out of five chamber locations used  
446 for evaluation. An improvement of the model could be achieved by a better representation of  
447 high water tables. The results from upscaling of CH<sub>4</sub> exchange show a net uptake of CH<sub>4</sub> of -10

448  $\mu\text{mol m}^{-2}\text{h}^{-1}$ . This is in contrast to gradient measurements above the canopy in the center of the  
449 study area, which yielded net  $\text{CH}_4$  emissions for the same time period (Sundqvist et al., 2015).  
450 Emissions were only found from 1.75 % of the surface of the study area. This suggests that the  
451 net emissions measured by the tower gradient method above the tree canopy probably originated  
452 from sources outside the study area and possibly also from  $\text{CH}_4$  emissions by the vegetation.  
453

454 **Acknowledgements**

455 Support for this work was provided by Formas, by the Linnaeus Centre LUCCI  
456 (<http://www.lucci.lu.se/index.html>) funded by the Swedish Research Council and by the EU  
457 project InGOS. We thank Anders Båth and Irene Lehner for field assistance. Airborne LiDAR  
458 for the Norunda site was acquired with support from the British Natural Environment Research  
459 Council (NERC/ARSF/FSF grant EU10-01 and NERC/GEF grant 933).

460

461

462



463 **References**

464 Beldring, S., Gottschalk, L., Seibert, J., and Tallaksen, L.M., 1999, Distribution of soil moisture  
465 and groundwater levels at patch and catchment scales: *Agricultural and Forest Meteorology*, v.  
466 98–99, p. 305-324.

467

468 Beven, K.J., and Kirkby, M.J., 1979, A physically based, variable contributing area model of  
469 basin hydrology: *Hydrol.Sci.Bull.*, v. 24, p. 43-69.

470

471 Boeckx, P., VanCleemput, O., and Villaralvo, I., 1997, Methane oxidation in soils with different  
472 textures and land use: *Nutrient Cycling in Agroecosystems*, v. 49, p. 91-95.

473

474 Buttle, J. M., P. J. Dillon, and G. R. Eerkes, 2004. Hydrologic coupling of slopes, riparian zones  
475 and streams: an example from the Canadian Shield. *Journal of Hydrology* 287:161-177

476

477 Castro, M.S., Melillo, J.M., Steudler, P.A., and Chapman, J.W., 1994, Soil-moisture as a  
478 predictor of methane uptake by temperate forest soils: *Canadian Journal of Forest Research-*  
479 *Revue Canadienne De Recherche Forestiere*, v. 24, p. 1805-1810.

480

481 Christensen, T.R., Ekberg, A., Strom, L., Mastepanov, M., Panikov, N., Oquist, M., Svensson,  
482 B.H., Nykanen, H., Martikainen, P.J., and Oskarsson, H., 2003, Factors controlling large scale  
483 variations in methane emissions from wetlands: *Geophysical Research Letters*, v. 30.

484

485 Christiansen, J.R., Vesterdal, L., and Gundersen, P., 2012, Nitrous oxide and methane exchange  
486 in two small temperate forest catchments-effects of hydrological gradients and implications for  
487 global warming potentials of forest soils: *Biogeochemistry*, v. 107, p. 437-454.  
488

489 Crill, P.M., Martikainen, P.J., Nykanen, H., and Silvola, J., 1994, Temperature and N-  
490 fertilization effects on methane oxidation in a drained peatland soil: *Soil Biology &*  
491 *Biochemistry*, v. 26, p. 1331-1339.  
492

493 Curry, C.L., 2007, Modeling the soil consumption of atmospheric methane at the global scale:  
494 *Global Biogeochemical Cycles*, v. 21.  
495

496 Del Grosso, S.J., Parton, W.J., Mosier, A.R., Ojima, D.S., Potter, C.S., Boroken, W., Brumme, R.,  
497 Butterbach-Bahl, K., Crill, P.M., Dobbie, K., and Smith, K.A., 2000, General CH<sub>4</sub> oxidation  
498 model and comparisons of CH<sub>4</sub> oxidation in natural and managed systems: *Global*  
499 *Biogeochemical Cycles*, v. 14, p. 999-1019.  
500

501 Dorr, H., Katruff, L., and Levin, I., 1993, Soil texture parameterization of the methane uptake in  
502 aerated soils: *Chemosphere*, v. 26, p. 697-713.  
503

504 Draper, N.R., and Smith, H., 1998, *Applied Regression analyses*, Wiley-Interscience, 307-312 p.  
505

506 Dunfield, P., Knowles, R., Dumont, R., and Moore, T.R., 1993, Methane production and  
507 consumption in temperate and sub-arctic peat soils-response to temperature and pH: *Soil Biology*  
508 & *Biochemistry*, v. 25, p. 321-326.  
509

510 Dutaur, L., and Verchot, L.V., 2007, A global inventory of the soil CH<sub>4</sub> sink: *Global*  
511 *Biogeochemical Cycles*, v. 21.  
512

513 Fiedler, S., Holl, B.S., and Jungkunst, H.F., 2005, Methane budget of a Black Forest spruce  
514 ecosystem considering soil pattern: *Biogeochemistry*, v. 76, p. 1-20.  
515

516 Fiedler, S., and Sommer, M., 2000, Methane emissions, groundwater levels and redox potentials  
517 of common wetland soils in a temperate-humid climate: *Global Biogeochemical Cycles*, v. 14, p.  
518 1081-1093.  
519

520 Fischer, J.C.v., and Hedin, L.O., 2002, Separating methane production and consumption with a  
521 field-based isotope pool dilution technique: *Global Biogeochemical Cycles*, v. 16, p. 8/1-8/13.  
522

523 Gauci, V., Gowing, D.J.G., Hornibrook, E.R.C., Davis, J.M., and Dise, N.B., 2010, Woody stem  
524 methane emission in mature wetland alder trees: *Atmospheric Environment*, v. 44, p. 2157-2160.  
525

526 Grayson, R.B., Western, A.W., Chiew F.H.S., 1997. Preferred states in spatial soil moisture  
527 patterns: Local and nonlocal controls. *Water Resources Research* 33: 2897–2908.  
528

529 Grip, H., and Rodhe, A., 1994, Vattnets väg från regn till bäck: Uppsala, Hallgren & Fallgren  
530 Studieförlag AB.  
531

532 Grunwald, D., Fender, A.C., Erasmi, S., and Jungkunst, H.F., 2012, Towards improved bottom-  
533 up inventories of methane from the European land surface: Atmospheric Environment, v. 51, p.  
534 203-211.  
535

536 Guckland, A., Flessa, H., and Prenzel, J., 2009, Controls of temporal and spatial variability of  
537 methane uptake in soils of a temperate deciduous forest with different abundance of European  
538 beech (*Fagus sylvatica* L.): Soil Biology & Biochemistry, v. 41, p. 1659-1667.  
539

540 Hamby, D.M., 1994, A review of techniques for parameter sensitivity analysis of environmental  
541 models: Environmental Monitoring and Assessment, v. 32, p. 135-154.  
542

543 Harriss, R.C., Sebacher, D.I., and Day, F.P., 1982, Methane flux in the great dismal swamp:  
544 Nature, v. 297, p. 673-674.  
545

546 Hashimoto, S., Morishita, T., Sakata, T., Ishizuka, S., Kaneko, S., and Takahashi, M., 2011,  
547 Simple models for soil CO<sub>2</sub>, CH<sub>4</sub>, and N<sub>2</sub>O fluxes calibrated using a Bayesian approach and  
548 multi-site data: Ecological Modelling, v. 222, p. 1283-1292.  
549

550 Heiskanen, J., and Makitalo, K., 2002, Soil water-retention characteristics of Scots pine and  
551 Norway spruce forest sites in Finnish Lapland: *Forest Ecology and Management*, v. 162, p. 137-  
552 152.

553

554 Hopkinson, C., Chasmer, L.E., Sass, G., Creed, I.F., Sitar, M., Kalbfleisch, W., and Treitz, P.,  
555 2005, Vegetation class dependent errors in lidar ground elevation and canopy height estimates in  
556 a boreal wetland environment: *Canadian Journal of Remote Sensing*, v. 31, p. 191-206.

557

558 Högstrom, U., 1988, Non-dimensional wind and temperature profiles in the atmospheric surface-  
559 layer- a re-evaluation: *Boundary layer meteorology*, **42**, 55-78.

560

561 Ku, H. H., 1966, Notes on the use of propagation of error formulas: *Journal of Research of the*  
562 *National Bureau of Standards (National Bureau of Standards) 70C (4): 262.*  
563 doi:10.6028/jres.070c.025. ISSN 0022-4316

564

565 Ishizuka, S., Sakata, T., Sawata, S., Ikeda, S., Sakai, H., Takenaka, C., Tamai, N., Onodera, S.,  
566 Shimizu, T., Kan-na, K., Tanaka, N., and Takahashi, M., 2009, Methane uptake rates in Japanese  
567 forest soils depend on the oxidation ability of topsoil, with a new estimate for global methane  
568 uptake in temperate forest: *Biogeochemistry*, v. 92, p. 281-295.

569

570 Jungkunst, H.F., Flessa, H., Scherber, C., and Fiedler, S., 2008, Groundwater level controls  
571 CO<sub>2</sub>, N<sub>2</sub>O and CH<sub>4</sub> fluxes of three different hydromorphic soil types of a temperate forest  
572 ecosystem: *Soil Biology & Biochemistry*, v. 40, p. 2047-2054.

573

574 Kammann, C., Grunhage, L., Jager, H.J., and Wachinger, G., 2001, Methane fluxes from  
575 differentially managed grassland study plots: the important role of CH<sub>4</sub> oxidation in grassland  
576 with a high potential for CH<sub>4</sub> production: *Environmental Pollution*, v. 115, p. 261-273.

577

578 Kammann, C., Hepp, S., Lenhart, K., and Muller, C., 2009, Stimulation of methane  
579 consumption by endogenous CH<sub>4</sub> production in aerobic grassland soil: *Soil Biology &*  
580 *Biochemistry*, v. 41, p. 622-629.

581

582 King, G.M., and Adamsen, A.P.S., 1992, Effects of temperature on methane consumption in a  
583 forest soil and in pure cultures of the methanotroph *Methylobacterium rubrum*: *Applied and*  
584 *Environmental Microbiology*, v. 58, p. 2758-2763.

585

586 Kirschke, S., 2013, Three decades of global methane sources and sinks: *Nature geoscience*, v. 6,  
587 p. 813-823.

588

589 Kljun, N., P. Calanca, M.W. Rotach, H.P. Schmid, 2004: A Simple Parameterisation for Flux  
590 Footprint Predictions. *Boundary-Layer Meteorology* v.112, p.503-523.

591

592 Konda, R., Ohta, S., Ishizuka, S., Arai, S., Ansori, S., Tanaka, N., and Hardjono, A., 2008,  
593 Spatial structures of N<sub>2</sub>O, CO<sub>2</sub>, and CH<sub>4</sub> fluxes from *Acacia mangium* plantation soils  
594 during a relatively dry season in Indonesia: *Soil Biology & Biochemistry*, v. 40, p. 3021-3030.

595

596 Koslowski, T.T., 1997, Responses of woody plants to flooding and salinity. *Tree Physiology*  
597 Monograph No. 1: Victoria, Canada., Heron Publishing.

598

599 Lamb, R., Beven, K., and Myrabø, S., 2001, Shallow Groundwater Response at Minifelt, *in*  
600 Grayson, R., and Blöschl, G., eds., *Spatial patterns in catchment hydrology*, Cambridge  
601 University Press, p. 272-303.

602

603 Lessard, R., Rochette, P., Topp, E., Pattey, E., Desjardins, R.L., and Beaumont, G., 1994,  
604 Methane and carbon-dioxide fluxes from poorly drained adjacent cultivated and forest sites:  
605 *Canadian Journal of Soil Science*, v. 74, p. 139-146.

606

607 Lin, H.S., Kogelmann, W., Walker, C., and Bruns, M.A., 2006, Soil moisture patterns in a  
608 forested catchment: A hydro pedological perspective: *Geoderma*, v. 131, p. 345-368.

609

610 Marushchak, M.E., Kiepe, I., Biasi, C., Elsakov, V., Friberg, T., Johansson, T., Soegaard, H.,  
611 Virtanen, T., and Martikainen, P.J., 2013, Carbon dioxide balance of subarctic tundra from plot  
612 to regional scales: *Biogeosciences*, v. 10, p. 437-452.

613

614 Matson, P.A., Vitousek, P.M., and Schimel, D.S., 1989, *Regional extrapolations of trace gas flux*  
615 *based on soils and ecosystems*, John Wiley, Dahlem Konferenzen;.

616

617 McNamara, N.P., Chamberlain, P.M., Pearce, T.G., Sleep, D., Black, H.I.J., Reay, D.S., and  
618 Ineson, P., 2006, Impact of water table depth on forest soil methane turnover in laboratory soil

619 cores deduced from natural abundance and tracer C-13 stable isotope experiments: Isotopes in  
620 Environmental and Health Studies, v. 42, p. 379-390.

621

622 Molénat, J., Gascuel-Oudou, C., Davy, P., and Durand, P., 2005, How to model shallow water-  
623 table depth variations: the case of the Kervidy-Naizin catchment, France: Hydrological  
624 Processes, v. 19, p. 901-920.

625

626 Moncrieff, J. B., Massheder, J.M., de Bruin, H., Elbers, J., Friborg, 1997, A system to measure  
627 surface fluxes of momentum, sensible heat, water vapor and carbon dioxide. Journal of  
628 hydrology **188-189**, 589-611.

629

630 Mölder, M., Grelle, A., Lindroth, A., and Halldin, S., 1999, Flux-profile relationships over a  
631 boreal forest - roughness sublayer corrections: Agricultural and forest meteorology, **98-9**, 645-  
632 658.

633

634 Nicoloni, G., Castaldi, S., Fratini, G., and Valentini, R., 2013, A literature overview of  
635 micrometeorological CH<sub>4</sub> and N<sub>2</sub>O flux measurements in terrestrial ecosystems: Atmospheric  
636 Environment, v. 81, p. 311-319.

637

638 Physick, W.L., and Garratt, J.R., 1995, Incorporation of a high-roughness lower boundary into a  
639 mesoscale model for studies of dry deposition over complex terrain: Boundary layer  
640 meteorology, **74**, 55-71.

641

642



643 Pilesjö, P., Persson, D.A., and Harrie, L., 2006, Digital Elevation Data for Estimation of  
644 Potential Wetness in Ridged Fields - Comparison of Two Different Methods: Agricultural Water  
645 Management, v. 79, p. 225-247.

646

647 Pilesjö, P., Zhou, Q., and Harrie, L., 1998, Estimating flow distribution over digital elevation  
648 models using a form-based algorithm: Geographic Information Sciences, v. 4, p. 44-51.

649

650 Polacek, D., Kofler, W., and Oberhuber, W., 2006, Radial growth of *Pinus sylvestris* growing on  
651 alluvial terraces is sensitive to water-level fluctuations: New Phytologist, v. 169, p. 299-308.

652

653 Reay, D.S., Nedwell, D.B., McNamara, N., and Ineson, P., 2005, Effect of tree species on  
654 methane and ammonium oxidation capacity in forest soils: Soil Biology & Biochemistry, v. 37,  
655 p. 719-730.

656

657 Ridgwell, A.J., Marshall, S.J., and Gregson, K., 1999, Consumption of atmospheric methane by  
658 soils: A process-based model: Global Biogeochemical Cycles, v. 13, p. 59-70.

659

660 Riley, W. J., Subin, Z.M., Lawrence, D.M., Swenson, S.C., Torn, M.S., Meng, L., Mahowald, N.M., and  
661 Hess, P., 2011, Barriers to predicting changes in global terrestrial methane fluxes: analyses using  
662 CLM4Me, a methane biogeochemistry model integrated in CESM. Biogeosciences 8:1925-1953.

663

664 Roulet, N., Moore, T., Bubier, J., and Lafleur, P., 1992, Northern fens-, methane flux and  
665 climatic-change: Tellus Series B-Chemical and Physical Meteorology, v. 44, p. 100-105.

666

667 Schimel, D.S., and Potter, C.S., 1995, Process modelling and spatial extrapolation *in* Matson,  
668 P.A., and Harriss, R.C., eds., Biogenic trace gases: Measuring emissions from soils and water:  
669 Cambridge, Blackwell Sci.,, p. 358-383.  
670

671 Schmidt, F., and Persson, A., 2003, Comparison of DEM Data Capture and Topographic  
672 Wetness Indices: Precision Agriculture, v. 4, p. 179-192.  
673

674 Seibert, J., Bishop, K.H., and Nyberg, L., 1997, A test of TOPMODEL'a ability to predict  
675 spatially distributed groundwater levels: Hydrological Processes, v. 11, p. 1131-1144.  
676

677 Steudler, P.A., Bowden, R.D., Melillo, J.M., and Aber, J.D., 1989, Influence of nitrogen-  
678 fertilization on methane uptake in temperate forest soils: Nature, v. 341, p. 314-316.  
679

680 Sundqvist, E., Crill, P., Molder, M., Vestin, P., and Lindroth, A., 2012, Atmospheric methane  
681 removal by boreal plants: Geophysical Research Letters, v. 39.  
682

683 Sundqvist, E., Mölder, M., Crill, P., Kljun, N., and Lindroth, A., Methane exchange in a boreal  
684 forest estimated by gradient method, Tellus B, 2015, 67, 26688,  
685

686 Sundqvist, E., Vestin, P., Crill, P., Persson, T., and Lindroth, A., 2014b, Short-term effects of  
687 thinning, clear-cutting and stump harvesting on methane exchange in a boreal forest,  
688 Biogeosciences, 11, 6095-6105  
689

690 Tenenbaum, D.E., Band, L.E., Kenworthy, S.T., Tague, C.L., 2006. Analysis of soil moisture  
691 patterns in forested and suburban catchments in Baltimore, Maryland, using high-resolution  
692 photogrammetric and LIDAR digital elevation datasets. *Hydrological*  
693 *Processes* 20: 219-240.

694

695 Tian, H., Xu, X., Liu, M., Ren, W., Zhang, C., Chen, G., and Lu, C., 2010, Spatial and temporal patterns  
696 of CH<sub>4</sub> and N<sub>2</sub>O fluxes in terrestrial ecosystems of North America during 1979-2008: application of a  
697 global biogeochemistry model. *Biogeosciences* 7:2673-2694.

698

699 Vigano, I., van Weelden, H., Holzinger, R., Keppler, F., McLeod, A., and Rockmann, T., 2008,  
700 Effect of UV radiation and temperature on the emission of methane from plant biomass and  
701 structural components: *Biogeosciences*, v. 5, p. 937-947.

702

703 Ward, A.D., and Trimble, S.W., 2004, *Environmental hydrology*, Lewis publisher.

704 Weslien, P., Klemedtsson, A.K., Borjesson, G., and Klemedtsson, L., 2009, Strong pH influence  
705 on N<sub>2</sub>O and CH<sub>4</sub> fluxes from forested organic soils: *European Journal of Soil Science*, v. 60, p.  
706 311-320.

707

708 Western, A.W., Grayson, R.B., Blöschl, G., Willgoose, G.R., and McMahon, T.A., 1999,  
709 Observed spatial organization of soil moisture and its relation to terrain indices: *Water Resources*  
710 *Research*, v. 35, p. 797-810.

711

712 Yu, K.W., Faulkner, S.P., and Baldwin, M.J., 2008, Effect of hydrological conditions on nitrous  
713 oxide, methane, and carbon dioxide dynamics in a bottomland hardwood forest and its  
714 implication for soil carbon sequestration: *Global Change Biology*, v. 14, p. 798-812.  
715

716 Yvon-Durocher, G., Allen, P.A., Bastviken, B., Conrad, R., Gudas, C., St-Pierre, A., Thanh-  
717 Duc, N., and Giorgio, P.A., 2014, Methane fluxes show consistent temperature dependence  
718 across microbial to ecosystem scales: *Nature*, v. 507, p. 488-491.  
719

720

721 Zhuang, Q., Melillo, J.M., Kicklighter, D.W., Prinn, R.G., McGuire, A.D., Steudler, P.A., Felzer, B.S.,  
722 and Hu, S., 2004, Methane fluxes between terrestrial ecosystems and the atmosphere at northern high  
723 latitudes during the past century: A retrospective analysis with a process-based biogeochemistry model.  
724 *Global Biogeochemical Cycles* 18:GB3010, doi:3010.1029/2004GB002239.

725 **Tables**

726 Table 1.

727 Soil temperature variability at Norunda. Here *Mean* and *Std* are the mean and standard  
728 deviation of the soil temperature respectively at *n* number of measurement locations within  
729 the study area. The measurements were taken in 2014.

730

	Mean (°C)	Std (°C)	n
July (undisturbed forest)	17.2	2.1	21
July (thinned forest)	17.9	1.4	12
September (undisturbed forest)	8.3	1.0	21
September (thinned forest)	7.8	0.9	12

731

732

733

734

735

736

737

738

739

740

741

742

743

744 Table 2

745 Evaluation of empirical models for upscaling of CH<sub>4</sub> exchange.

746 ID is the combination of chambers used for model development. R<sup>2</sup> is the adjusted coefficient of  
 747 determination for the multiple linear regression analyses between model and chamber input data.

748 B(T), B(W) and B(SM) are the coefficients for soil temperature, water table depth and soil

749 moisture, respectively, obtained from the multiple linear regression analyses. I is the regression

750 intercept. R is the Pearson correlation coefficient for modelled CH<sub>4</sub> exchange and chamber data.

751 \*) Not significant at p >0.05. n.i ) Not included due to non-significance. -) Chamber was used for

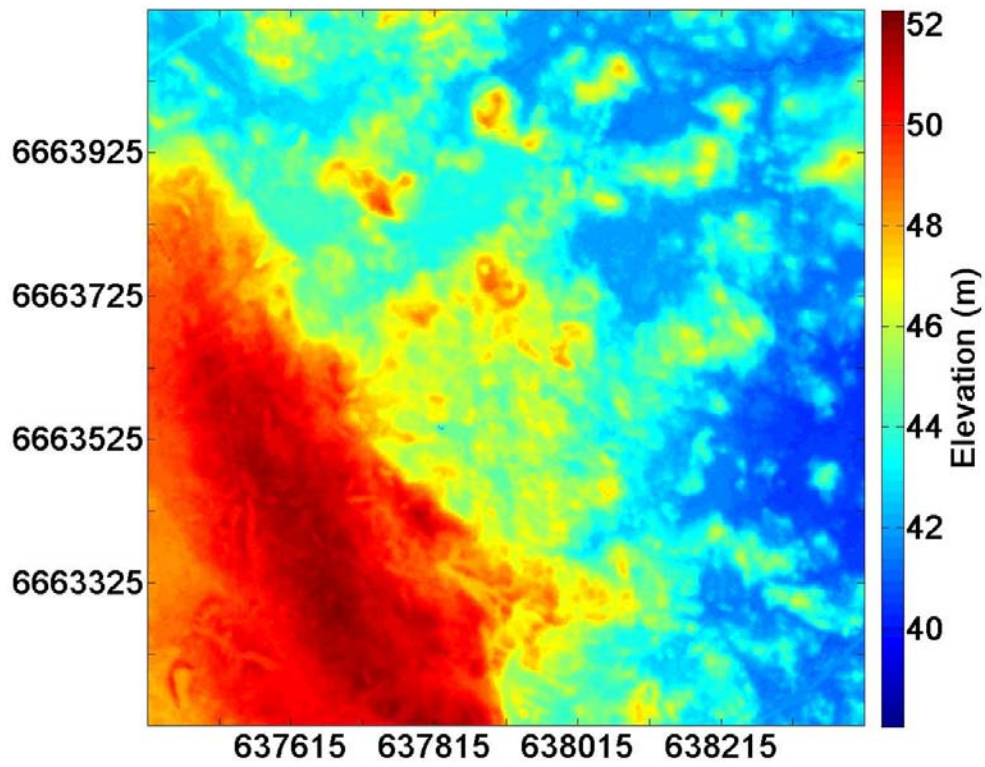
752 model development and is therefore not evaluated.

753

ID	R <sup>2</sup>	B (T)	B (W)	B (SM)	I	R (U1)	R (U2)	R (U3)	R (U4)	R (U5)	R (T1)	R (T2)	R (T3)
U4, U5, T1	0.68	-0.43	5.8	n.i	4.8	0.79	0.79	0.81	-	-	-	0.71	-0.33*
U4, U3, T1	0.80	-0.31	3.1	0.08	3.7	0.80	0.78	-	-	0.96	-	0.63	-0.43*
U4, U2, T1	0.58	-0.30	1.9	0.09	-6.3	0.85	-	0.87	-	0.94	-	0.48	0.13
U4, U2, T1	0.55	-0.42	7.2	n.i	7.2	-	0.78	0.81	-	0.94	-	0.71	-0.21*
U4, U5, T2	0.71	-0.20	2.2	0.03	-4.6	0.84	0.74	0.88	-	-	0.62	-	-0.09*
U4, U3 T2	0.80	-0.32	3.5	0.08	-2.8	0.85	0.72	-	-	0.94	0.68	-	0.15*
U4, U2, T2	0.57	-0.33	3.6	0.05	-2.4	0.84	-	0.88	-	0.96	0.62	-	-0.09*
U4, U1, T2	0.54	-0.46	6.0	n.i	5.8	-	0.79	0.81	-	0.95	0.41	-	-0.34*
U4, U5, T3	0.56	n.i	8.1	0.16	0.60	0.69	0.61	0.74	-	-	0.08	-0.03*	-
U4, U3, T3	0.54	n.i	6.8	0.22	-4.6	0.71	0.58	-	-	0.67	0.58	-0.04*	-
U4, U2, T3	0.52	0.40	4.5	0.30	-15.3	0.43	-	0.36	-	0.18*	0.47	-0.23*	-
U4, U1, T3	0.53	n.i	8.9	0.15	2.3	-	0.62	0.74	-	0.68	0.54	-0.02*	-
U5, U3, T1	0.51	-0.37	n.i	0.05	-5.9	0.81	0.66	-	0.83	-	-	0.52	-0.46*
U5, U2, T1	0.28	-0.39	n.i	0.03	-5.7	0.80	-	0.72	0.80	-	-	0.52	-0.53*
U5, U1, T1	0.58	-0.49	4.7	-0.03	5.7	-	0.79	0.73	0.82	-	-	0.62	-0.53*
U5, U3, T2	0.53	-0.39	n.i	0.06	-5.7	0.81	0.65	-	0.83	-	0.41	-	-0.42*
U5, U2, T2	0.30	-0.42	1.3	n.i	-2.7	0.78	-	0.74	0.80	-	0.19	-	-0.57*
U5, U1, T2	0.59	-0.51	2.6	n.i	2.2	-	0.75	0.77	0.83	-	0.24	-	-0.54*
U5, U3, T3	0.44	n.i	n.i	0.32	-15.1	0.64	0.44	-	0.52	-	0.59	-0.06*	-
U5, U2, T3	0.39	n.i	n.i	0.33	-16.1	0.64	-	0.51	0.52	-	0.59	-0.06*	-
U5, U1, T3	0.48	n.i	3.4	0.24	-6.9	-	0.53	0.62	0.65	-	0.60	-0.05*	-
U3, U2, T1	0.50	-0.17	2.9	0.08	6.5	0.83	-	-	0.90	0.89	-	0.31	0.53
U3, U1, T1	0.25	-0.40	-1.6	0.03	-6.7	-	0.57	-	0.67	0.80	-	0.46	-0.56*
U3, U2, T2	0.49	-0.19	4.6	0.05	-3.1	0.80	-	-	0.93	0.89	0.66	-	0.37
U3, U1, T2	0.29	-0.42	-1.8	0.05	-7.0	-	0.57	-	0.70	0.81	0.26	-	0.53
U3, U2, T3	0.53	0.35	12.0	0.21	-3.4	-0.43*	-	-	-0.49*	-0.78*	0.25	-0.39*	-
U3, U1, T3	0.37	n.i	n.i	0.30	-14.2	-	0.44	-	0.52	0.51	0.59	-0.06*	-
U2, U1, T1	0.16h	-0.44	n.i	n.i	-3.8	-	-	0.68	0.72	0.87	-	0.50	-0.59*
U2, U1, T2	0.19	-0.46	n.i	n.i	-3.5	-	-	0.68	0.72	0.87	0.13	-	-0.59*
U2, U1, T3	0.35	n.i	5.7	0.20	-4.8	-	-	0.69	0.73	0.66	0.59	-0.04*	-

754

755 **Figures**  
756  
757



771 Figure 1. Digital Elevation Model (DEM) of the study area. Coordinates are given in UTM  
772 (WGS 84).

773

774

775

776

777

778

779

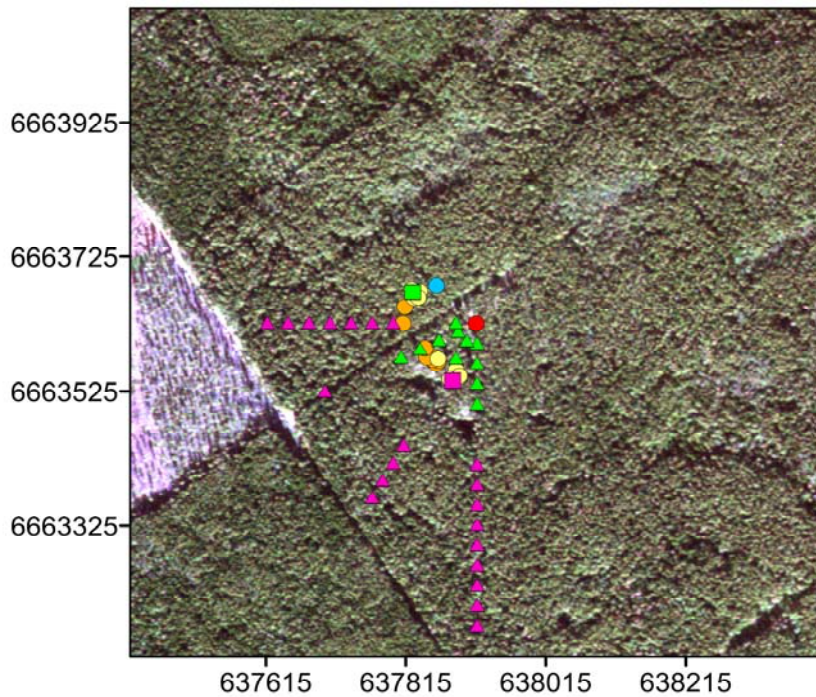
780

781

782

783

784



- Chamber measurements, thinned forest
- Chamber measurements, undisturbed forest
- Gradient measurements
- Water table measurements
- Soil moisture measurements 2010
- Soil moisture measurements 2013
- ▲ Soil temperature measurements, undisturbed forest
- ▲ Soil temperature measurements, thinned forest

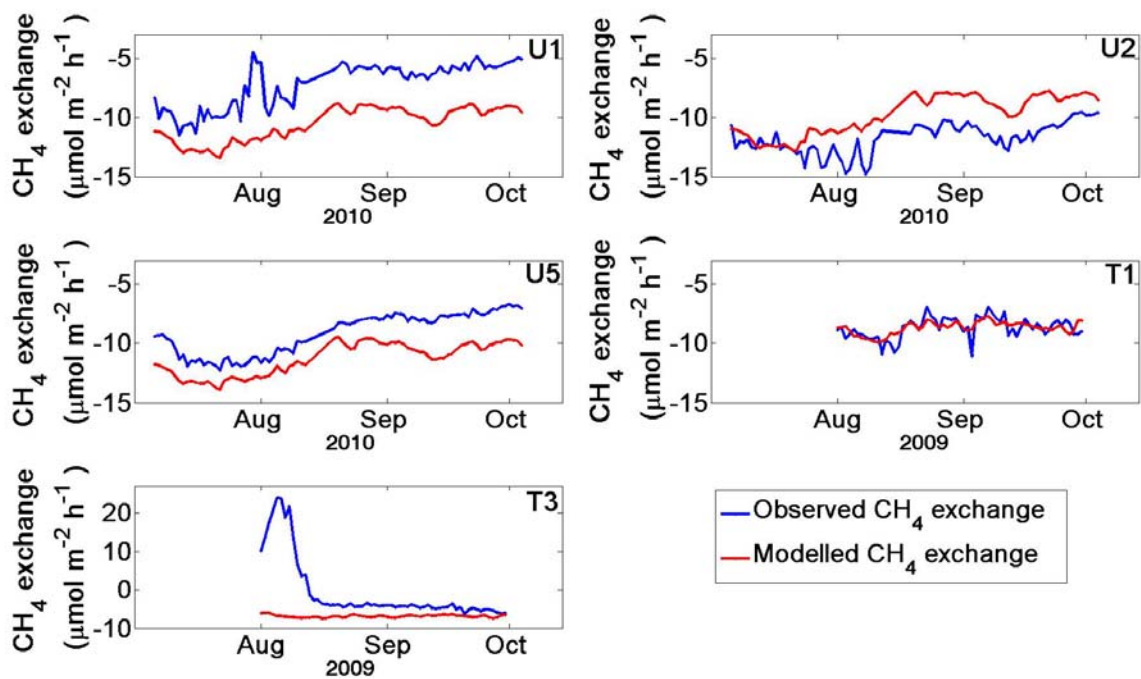
785  
786

787 Figure 2. Photo of the study area showing locations for chamber measurements, soil moisture  
788 measurements, water table measurements and gradient measurements. The clear-cut can be seen  
789 to the left.

790 (Source: Geoeye-1© GeoEye Inc.<2009> Distributed by e-GEOS)

791  
792





793 Figure 3. Comparison between modelled and observed CH<sub>4</sub> exchange for the evaluation  
 794 chambers. Ux are chambers in the undisturbed forest and Tx are chambers in the thinned forest.  
 795

796

797

798

799

800

801

802

803

804

805

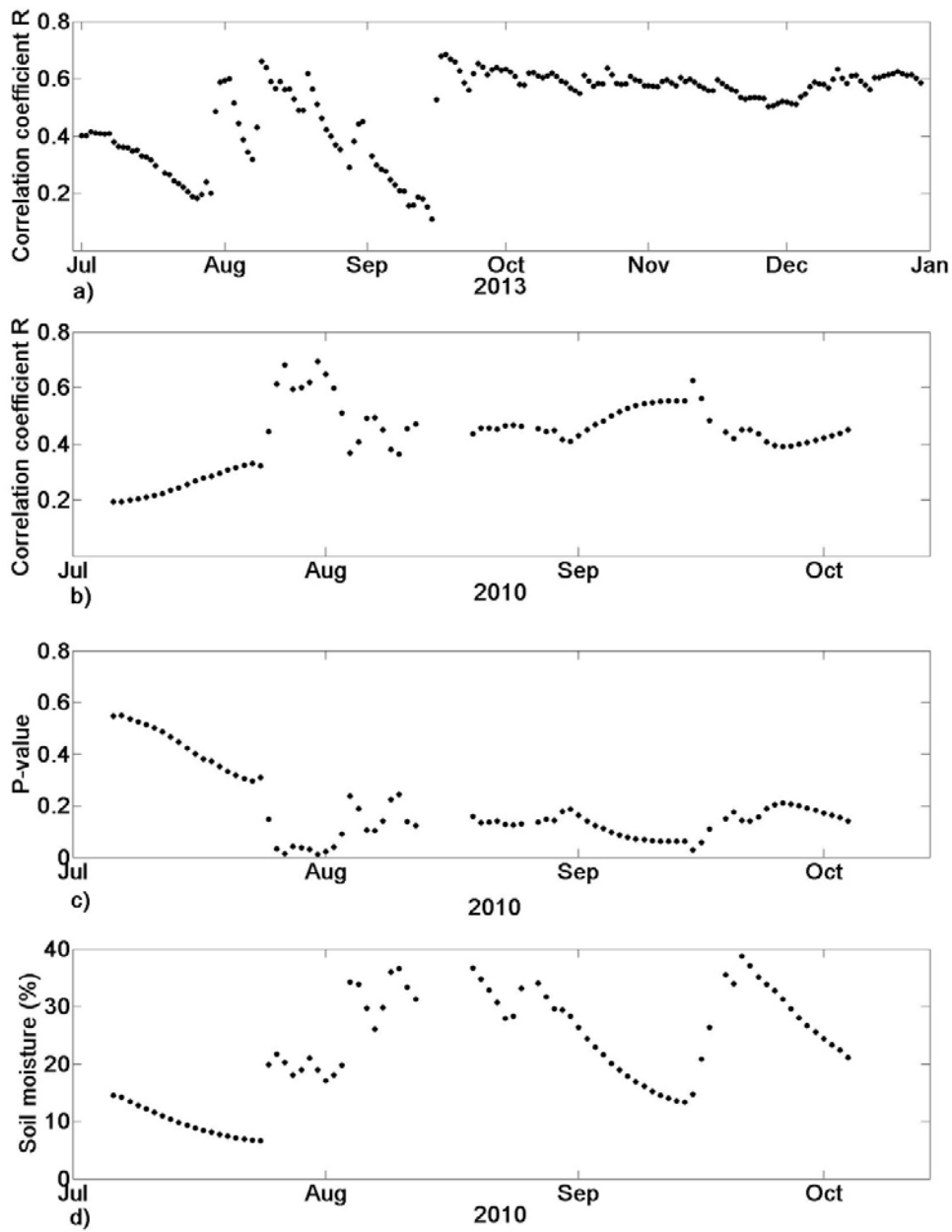
806

807

808

809

810



811

812

813

814

815

816

817 Figure 4. Average daily Pearson correlation between TWI and soil moisture measured at a) 9

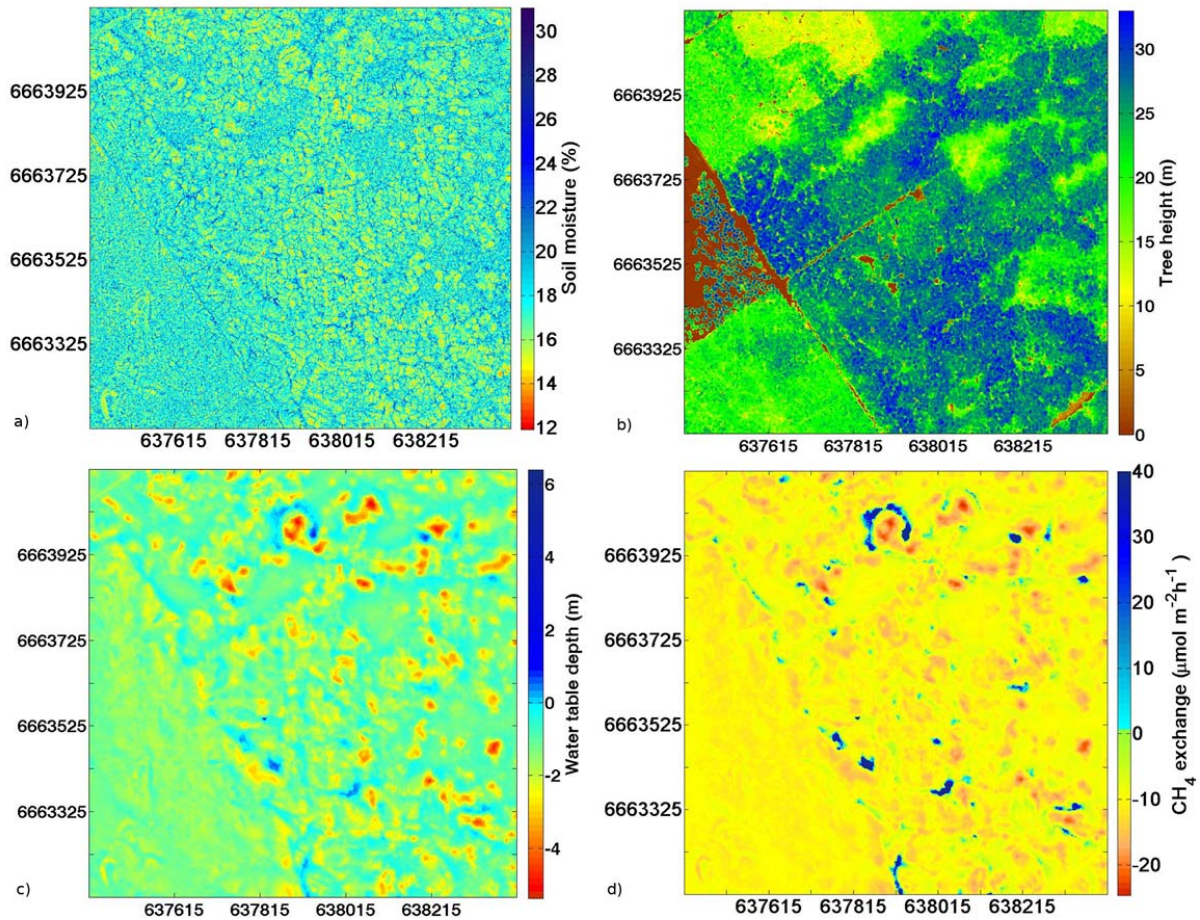
818 locations July- December 2013; and b) 12 locations July-October 2010; Daily significance level

819 for correlations between c) TWI and soil moisture measured at 12 locations July-October 2010;

820 and d) daily soil moisture at one measurement location for the time period July-October 2010.

821

822  
823  
824  
825

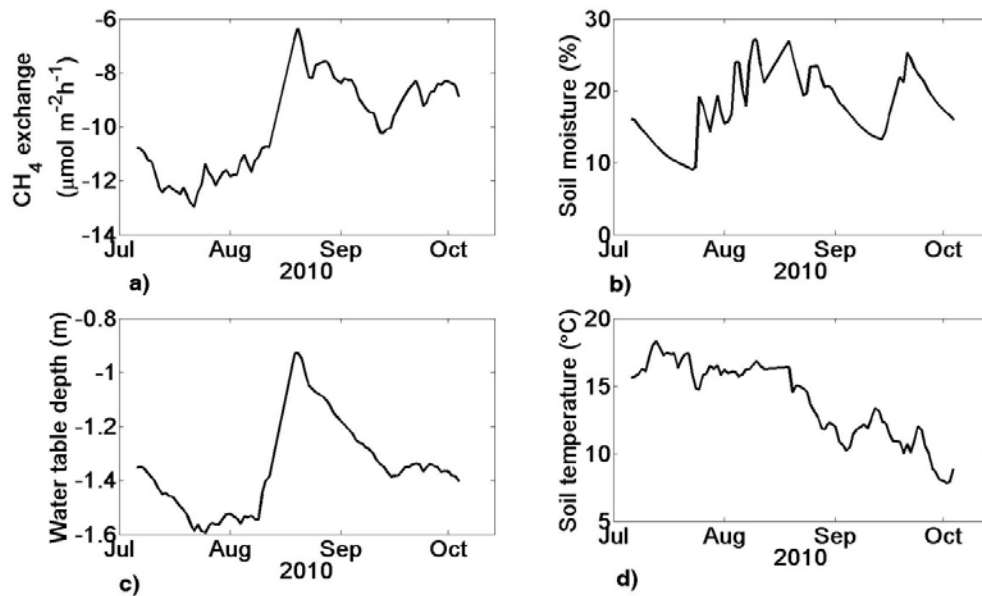


826  
827  
828  
829

830 Figure 5. a) Map of soil moisture for the entire study area, averaged over the study time period  
831 July through September 2010. b) Map of tree height in the study area. c) Map of water table  
832 depth for the study area, averaged over the study time period. d) Map of modelled CH<sub>4</sub> exchange  
833 for the study area, averaged over the study time period. Coordinates are given in UTM (WGS  
834 84).

835  
836

837  
838  
839  
840  
841  
842



843  
844  
845 Figure 6. Time series of modelled a) CH<sub>4</sub> exchange, b) soil moisture, c) water table depth and d)  
846 soil temperature, spatially averaged over the study area.